



Iron speciation in volcanic topsoils from Fogo island (Cape Verde) – Iron oxide nanoparticles and trace elements concentrations



R. Marques^{a,c}, J.C. Waerenborgh^{a,d}, M.I. Prudêncio^{a,c,*}, M.I. Dias^{a,c}, F. Rocha^{b,c}, E. Ferreira da Silva^{b,c}

^a Campus Tecnológico e Nuclear, IST/ITN, Instituto Superior Técnico, Universidade Técnica de Lisboa, Estrada Nacional 10, 2686-953 Sacavém, Portugal

^b Departamento de Geociências, Univ. de Aveiro, Aveiro, Portugal

^c GeoBioTec, Univ. de Aveiro, Aveiro, Portugal

^d Centro de Física da Matéria Condensada, Univ. de Lisboa, Portugal

ARTICLE INFO

Article history:

Received 10 April 2013

Received in revised form 19 July 2013

Accepted 27 September 2013

Keywords:

Iron speciation

Nanoparticles

Volcanic topsoils

Semi-arid environment

Fogo island, Cape Verde

ABSTRACT

Iron contents, its compounds and forms in topsoils of the volcanic Fogo island (Cape Verde) were studied by neutron activation analysis, Mössbauer spectroscopy and X-ray diffraction. The topsoils were collected from all units of the island in diverse geological formations – carbonatite, nephelinites, limburgite, pyroclasts, deposits, pre-historic lavas and historic lavas. Fine materials from Mota Gomes volcanic crater (the most recent eruption which occurred in 1995) were also sampled. The total iron content varies significantly from 1.7% (Fe₂O₃ weight) in acid sulfate topsoils (pH = 3.9), up to between 9.9% and 20.6% in the other geological contexts (pH = 5.9 to 9.3).

The most oxidized topsoils from the pre-caldera formations are the oldest ones, as expected, while the reverse is observed for the post-caldera topsoils. In the latter case fast weathering of the lava outer layers, which have a higher glass component, may explain this observation. After erosion periods of 50–200 years significant amounts of the highly oxidized small particles are removed. The inner part of the lava, less oxidized, is then exposed and more slowly weathered than the former outer layers. Topsoils from pre-caldera formations derived from the more weather-resistant inner layers are also strongly altered since they have been exposed for periods of time several orders of magnitude longer than the post-caldera ones. In topsoils Fe²⁺ mainly occurs in pyroxenes, phyllosilicates and pure or slightly oxidized magnetite. With increasing age the (Fe²⁺)/(total Fe) ratio of the pre-caldera topsoils gradually decreases down to 4% indicating that the iron that is still incorporated in the silicates structures is increasingly oxidized. Maghemite is detected instead of magnetite and hematite appears, becoming the main Fe-containing phase in the oldest materials. These results suggest that in a first weathering step Fe²⁺ is oxidized within the silicates structure and within magnetite which gradually evolves to maghemite. With the eventual decomposition of silicates Fe³⁺ is remobilized in hematite. As weathering proceeds maghemite is also replaced by hematite. Goethite was not detected by Mössbauer spectroscopy, which may be explained by the aridity of the island. Iron in jarosite was identified by Mössbauer spectroscopy in topsoils developed on volcanic conduits. The presence of this mineral in alkaline surficial environments may be explained by a hypogene origin and stability over at least a few hundred years in the surficial environments of the semi-arid Fogo island. Contents of Cr and As that are potentially harmful to health increase with the concentration of nanosized Fe oxides. This correlation may be related to their high specific surface area.

© 2013 Elsevier B.V. All rights reserved.

1. Introduction

Weathering and soil characteristics are controlled by the drainage conditions of the profile and depend on the climate (rainfall and temperature), topography, nature of rock (fissural system, texture and

composition), and influence of the biosphere (Chesworth, 1992; Formoso, 2006; Gauthier-Lafaye et al., 1993; Holdsen and Berner, 1979; Marques et al., 2012; Meunier, 2003; Prudêncio et al., 2002, 2007, 2010, 2011). Mineral composition is of prime importance in weathering. Some minerals, such as quartz, are very stable. In contrast decomposition of olivine, plagioclases and pyroxenes starts almost as soon as the rock is exposed to weathering agents. The texture of the rock is also relevant since porosity and permeability facilitate exposure to these agents. Temperature and precipitation, including the precipitation distribution over time, runoff percent and evaporation rate, are the chief climatic controls of weathering. The rate at which weathering

* Corresponding author at: Campus Tecnológico e Nuclear, IST/ITN, Instituto Superior Técnico, Universidade Técnica de Lisboa, Estrada Nacional 10, 2686-953 Sacavém, Portugal. Tel.: +351 219946223; fax: +351 219946185.

E-mail address: iprudenc@ctn.ist.utl.pt (M.I. Prudêncio).

processes decompose and break down a solid rock body depends also on the surface area exposed to the atmosphere (Gordon and Dorn, 2005).

Volcanic rocks are fine-grained and minerals highly susceptible to chemical weathering, such as calcium plagioclases, olivine and pyroxene, are often present in significant amounts; moreover glassy components common in lava flows weather faster than crystalline phases. The surfaces of lava flows are generally vesicular and very porous, and the interior of the rock bodies is usually broken. Therefore lava flows are highly permeable and susceptible to decomposition.

In general, the weathering rates of volcanic materials slow down with increasing rock age. During weathering some elements are immobile, tied up in secondary minerals such as clays and oxides or their amorphous precursors. Among major elements, iron has a conservative behavior (immobile) along with Ti and Al (Carrol, 1970).

Most volcanic soils contain an abundance of iron which occurs in living systems as a minor element. Iron is however an essential constituent of these systems, in particular of a number of cellular enzymes, notably those associated with respiration processes. The physiologies of living organisms combine with chemical, physical, and geological forces to continually redistribute iron between living and non-living reservoirs in processes known as biogeochemical cycles. Among the elements which have variable oxidation states, iron is the most important in weathering reactions on earth (Berner and Berner, 1996; Summons, 1993). Oxidation is thus especially important in the weathering of minerals that have high iron content, such as olivine and pyroxene. When iron is oxidized, the change in valence and ionic radius causes destabilizing adjustments in the crystal structure of these minerals, facilitating bond breakage. Iron oxides are the main residual minerals of olivine and pyroxene weathering. On the other hand oxidation of primary iron oxides like magnetite also occurs and in the end hematite is expected to dominate particularly in arid environments. Among iron-bearing mineral phases, iron oxides are soil constituents of great interest in soil chemistry and relevance to plant nutrition. They have significant effects on many processes such as sorption and redox ones because of their high specific surface areas and reactivity, particularly when present as micro and nanosized particles. Furthermore, iron oxides are known to incorporate chemical elements that can be a threat to health (O'Day, 2006; Vaughan, 2006).

A generally high total iron content (mean $\text{Fe}_2\text{O}_3 = 14.1\%$; median = 14.3%) was found by Marques et al. (2012) in 63 topsoils of Santiago island (Cape Verde). Spatial variations of features of these topsoils were found to be significant in a small scale. A still higher variation may be expected for Fogo island, the only volcanic island of the Cape Verde archipelago which is presently active. In the present work the iron content and speciation in topsoils of this island are reported. The study is performed on whole sample (<2 mm fraction) of topsoils developed on volcanic rocks of different ages including surficial materials collected inside the Mota Gomes (MG) crater, which corresponds to the most recent volcanic eruption (1995). In order to evaluate the role of the iron forms, particularly iron oxide particles, in the sorption of potentially harmful chemical elements, chromium and arsenic contents were also determined.

In soils Fe is distributed among a variety of different species of mainly very small particle size which escape detection by XRD, particularly when it is performed in the <2 mm fraction as in the present study. Chemical analysis is also generally insufficient to an unambiguous determination of the individual Fe forms, as the species are only minor constituents within the very complex soil matrix. Combined with XRD and chemical analysis, ^{57}Fe Mössbauer spectra of the natural Fe species supply the best solution to the problem. Spectra are generally unique and characteristic for each individual chemical form. The parameters that allow the identification of the different Fe oxides are related to their magnetic properties. When the particle size of these oxides is very small these properties are only observed in the Mössbauer spectra at very low temperatures. This methodology was therefore adopted in the present study.

The main goals of this work are evaluating (1) the iron distribution in mineralogical phases of topsoils developed on volcanic rocks with different ages (from ~5 Ma down to a few decades) of the Fogo island (Cape Verde); (2) the ratio of $\text{Fe}^{3+}/\text{FeT}$ (where FeT stands for total Fe) within and between the different geological units; and (3) the particle size of iron oxides and its correlation with potentially health harmful elements such as Cr and As. This study is part of a broader project, for the establishment of an environmental geochemical atlas of the Cape Verde archipelago (Cabral Pinto, 2010; Marques et al., 2012).

2. Geological setting

Fogo island is the fourth largest island (476 km² area) of the Cape Verde archipelago (Fig. 1a), and is located in the south-western part of this archipelago, some 800 km off the Africa coast. Fogo is one of the youngest (~5 Ma) and seismically most active island in Cape Verde (Le Bas et al., 2007). This island is described as a relatively simple volcano-island, corresponding to an active volcano with a maximum altitude of 2829 m. All the archipelago origin is associated to the volcanic activity of an underlying mantle plume (Madeira et al., 2008).

The climate of Fogo island ranges from tropical to semi-arid with an average temperature of 25 °C. However, in Chã das Caldeiras the temperature may be as low as 0 °C in December and January (Mota Gomes, 2006). A high annual variability in precipitation may occur. The humid region (>600 mm/a) is located in the north-east, and arid regions (~160 mm/a) are in the south-west part of the island. Above 1300 m, a lower rainfall occurs due to the trade wind inversion (Olehowski et al., 2008). Several studies have been done in Fogo island concerning the volcanic activity (Brum da Silveira et al., 1996; Figueiredo et al., 1997, 1999; Heleno da Silva et al., 1999; Heleno et al., 2006), geomorphic and structural studies (Brum da Silveira et al., 2006; Day et al., 1999; Madeira and Brum da Silveira, 2005), geo-ecological studies (Olehowski et al., 2008), and the geochemistry and mineralogy of topsoils and paleosols (Marques et al., 2010, 2011a,b).

The pre-caldera formations of Fogo island include two stratigraphic units: (i) a carbonatite unit exposed in fluvial valleys and (ii) nephelinites and associated lavas (hereafter referred to as nephelinites) with layers of scoria or tuffs, previous to the formation of the caldera. The post-caldera formations (the third stratigraphic unit) include pre-historic or non-identified sequences as well as several historic eruptions (Madeira and Brum da Silveira, 2005; Madeira et al., 2005) and contemporaneous deposits. Lahar and slope deposits are also post-caldera formations although their precise age is not known. The remaining pyroclastic deposits are dated in Torres et al. (1998).

The grain size distribution of topsoils of Fogo varies significantly from coarse materials to silty-loam soils with no cohesion and a higher susceptibility to wind erosion.

3. Materials and methods

In 2009/2010 field work was performed in the Fogo island (Cape Verde) with the purpose of collecting surficial soil/regolith samples of the three stratigraphic units referred above in the geological setting section: two precaldera (carbonatite and nephelinite units) and the post-caldera formations. For this work 18 topsoil samples were selected (Fig. 1b, Table 1): five topsoils developed in rocks of the pre-caldera formations — one carbonatite, three nephelinites and one limburgite; and 13 topsoils developed in the rocks of the post-caldera formations (basanites, tephrites, phonotephrites, pyroclasts and deposits) — nine lavas and pyroclasts from historic eruptions, two pyroclasts non dated (pre-historic or historic eruptions previous to 1721) and two deposits contemporaneous of the post-caldera episodes corresponding to torrential or lahar (Table 1, Fig. 2). It should be noted that two of the post-caldera formations include the surficial materials collected inside the Mota Gomes crater, which corresponds to the most recent volcanic eruption (1995): one red (7.5R/3/8) and one yellow (2.5Y/8/4) topsoils

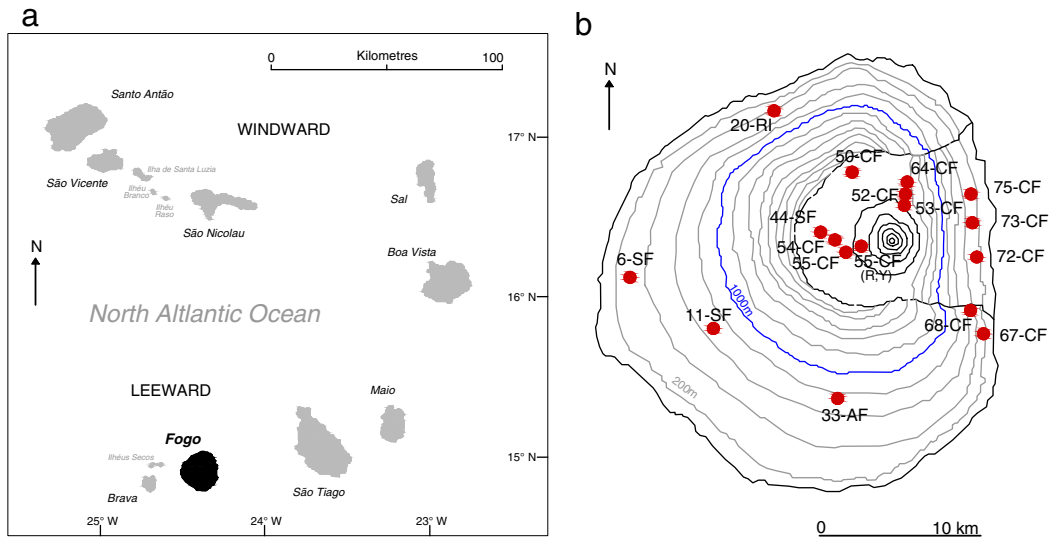


Fig. 1. a) Location of Fogo island (Cape Verde). b) Sampling location of 18 selected topsoils of the Fogo island, Cape Verde.

(Munsell, 1998). In general the topsoils from the pre-caldera formations are finer than those from the post-caldera.

The whole sample of the topsoils was obtained by sieving through a 2 mm aperture nylon mesh sieve. All the samples were air-dried and the pH was determined in a 5:1 water/soil suspension, by a pH meter scan 25 CW.

The topsoil samples were grounded in agate mortar for mineralogical and chemical analyses. The mineralogical composition of the whole sample was determined by X-ray diffraction (XRD) of randomly oriented specimens using a Philips diffractometer, Pro Analytical, with Cu K α radiation at 45 kV and 40 mA, a step size of 0.5° 2 θ /min from 3° to 70° 2 θ . Mineral identification was done according to Brindley and Brown (1980).

The total contents of Fe, Cr and As were obtained by instrumental neutron activation analysis (INAA). Two reference materials were used in the estimation of concentrations by INAA: soil GSS-4 and sediment GSD-9 from the Institute of Geophysical and Geochemical Prospecting (IGGE). Reference values were taken from data tabulated by Govindaraju (1994). The samples and standards were prepared for analysis by weighing 200–300 mg of powder into cleaned high-density polyethylene vials. Irradiations were performed in the core grid of the Portuguese Research Reactor (Sacavém) (Dung et al., 2010). More

details of the analytical method are given in Dias and Prudêncio (2007), Gouveia et al. (1992), Gouveia and Prudêncio (2000) and Prudêncio (2009).

The ^{57}Fe Mössbauer measurements were recorded at 295 K and 4.2 K in transmission mode using a conventional constant acceleration spectrometer and a 25-mCi ^{57}Co source in Rh matrix. The velocity scale was calibrated using an $\alpha\text{-Fe}$ foil at room temperature. Isomer shift values, IS, are given relative to this standard. Powdered samples were packed together with lucite powder into perspex holders, in order to obtain homogeneous and isotropic Mössbauer absorbers containing about 5 mg/cm 2 of natural iron. Measurements at 4.2 K were performed using a bath cryostat with the sample immersed in liquid He. The spectra were fitted to Lorentzian lines using a non-linear least-square method (Waerenborgh et al., 2003).

4. Results

4.1. pH and chemical composition

The water/soil suspension pH found in topsoils varies in general from slightly to strongly alkaline (Table 1), except in the Mota Gomes crater materials. The pH values of the topsoils from the pre-caldera

Table 1

Sample references, parent rock, chronology, pH, total iron (as oxide), chromium and arsenic contents of the studied topsoils of the Fogo island (Cape Verde). The dates and parent rock of the post-caldera formations samples are according Torres et al. (1998).

	Reference	Parent rock	Date	pH	Fe $_2\text{O}_3\text{T}$ (%)	Cr (mg/kg)	As (mg/kg)	
Post-caldera formations	73-CF	Deposit (de/lahar)	Contemporaneous of the	7.9	12.2	15.8	n.d.	
	72-CF	Deposit (de/lahar)	post-caldera episodes	7.7	14.0	77.8	n.d.	
	55-CF Y	Pyroclasts (MG crater)	1995	3.9	1.7	11.2	13.5	
	55-CF R	Pyroclasts (MG crater)	1995	6.2	14.5	77.9	n.d.	
	55-CF	Pyroclasts	1995	5.9	10.5	59.3	n.d.	
	54-CF	Lava	1995	9.3	12.9	55.2	n.d.	
	44-SF	Lava	1995	9.3	9.9	19.2	n.d.	
	68-CF	Lava	1951	6.8	12.5	75.9	n.d.	
	50-CF	Lava	1951	8.7	12.8	47.8	n.d.	
	64-CF	Pyroclasts	1852	8.2	13.4	53.2	n.d.	
	75-CF	Lava	1799	8.8	11.0	51.6	n.d.	
	53-CF	Pyroclasts (volcanic conduit)	Before 1721	8.0	13.9	125	1.4	
	52-CF	Pyroclasts	Before 1721	8.2	13.4	99.1	n.d.	
	Pre-caldera formations	20-RI	Limburgite	–	7.8	18.5	382	0.709
		33-AF	Nephelinites	–	7.2	20.6	253	2.77
67-CF		Nephelinites	–	7.4	14.2	176	4.87	
11-SF		Nephelinites	–	7.6	17.0	197	1.95	
6-SF		Carbonatite	~5 Ma	9.1	12.1	41.1	0.838	

n.d. – non detected.



Fig. 2. Photographs of some studied topsoils of Fogo island (Cape Verde) from pre-caldera formations (33-AF, 11-SF, 67-CF) and from post-caldera formations (52-CF, 75-CF, 54-CF, 55-CF Y and R, 73-CF) (see Table 1 for sample description).

formations are slightly alkaline ($\text{pH} = 7.2\text{--}7.8$) with the exception of the carbonatite topsoil which is very strongly alkaline ($\text{pH} = 9.1$). In the post-caldera formations, the pH range is $6.8\text{--}9.3$, with the main difference found for the fine materials of the MG crater, where the pH values are acidic, even extremely acidic ($\text{pH} = 3.9$) for the yellow 55-CF Y sample.

The chemical results obtained for Fe, Cr and As in the studied topsoils of Fogo island are given in Table 1. Despite the high Fe and Cr contents found, the values are within the range referred for soils throughout the world (Bowen, 1979). Arsenic contents are low, except in the yellow materials collected inside the MG crater. Some significant differences were found concerning the Fe contents, the highest value occurs in the pre-caldera formations (topsoil 33-AF, nephelinite) and the lowest content in the yellow sample collected in MG crater (post-caldera formations). The Cr contents vary significantly and the highest values were found in the pre-caldera topsoils (176–382 mg/kg), with exception of the carbonatite (41 mg/kg); in the post-caldera formations a high content of Cr occurs in the topsoil of the older volcanic conduit studied (53-CF, before 1721). The same tendency occurs for arsenic: the higher contents of this element were detected in the pre-caldera formations; in the post-caldera formations the As is not detected by INAA in the majority of the topsoils, except in the sample 53-CF (volcanic conduit, before 1721). The yellow pyroclastic

material from MG crater behaves differently, where the highest As content was observed in spite of the low Cr content.

4.2. Mineralogy

The low crystallinity and the presence of a vitreous component in the whole sample of the topsoils from Fogo island, observed as a bulge in the diffractogram baselines, make it difficult to determine the mineralogical composition by XRD. The results indicate that the most abundant minerals in the crystalline phase are pyroxenes (augite), particularly in the post-caldera formations (Table 2). The topsoil developed in the carbonatite unit is mainly composed by calcite, as expected in this kind of material. Also quartz, fluorapatite, phyllosilicates, K-feldspars, anatase and rutile occur. One of the topsoils developed in the nephelinites (33-AF, the sample with the highest FeT content) shows a distinct mineralogical composition, with the hematite as dominant mineral. In this sample in addition to pyroxenes and quartz, phyllosilicates were also detected. The limburgite topsoil (20-RI) has a different mineralogy with the presence of olivines as main mineral. Traces of fluorapatite, along with pyroxenes, phyllosilicates and quartz also occur.

In the post-caldera formations, a variety of mineralogical assemblages occurs, pyroxenes being the dominant mineral. However, in the MG crater samples, where evaporate minerals were found, gypsum

Table 2

Sample references and mineralogical associations obtained by XRD of the studied topsoils of the Fogo island (Cape Verde).

	Reference	Mineralogical association	Vitreous component	
Post-caldera formations	73-CF	Pyroxenes > Hematite > Phyllosilicates ≫ Quartz	+	
	72-CF	Pyroxenes > Hematite > Phyllosilicates > Fluorapatite > Analcime	–	
	55-CF Y	Gypsum ≫ Quartz ≫ Plagioclase (traces)	–	
	55-CF R	Gypsum ≫ Pyroxenes > Jarosite > Hematite > Phyllosilicates	–	
	55-CF	Pyroxenes ≫ Hematite ≈ Jarosite > Olivines > Maghemite/magnetite > Quartz	++	
	54-CF	Pyroxenes ≫ Hematite > Fluorapatite > Rutile (traces?)	+	
	44-SF	Pyroxenes ≫ K-Feldspars > Hematite > Fluorapatite > Maghemite–Phyllosilicates (traces)	+	
	68-CF	Pyroxenes ≫ Hematite > Quartz > Phyllosilicates > Fluorapatite > Magnetite/Maghemite?	+	
	50-CF	Pyroxenes > Hematite > Magnetite/Maghemite > Olivines > Phyllosilicates (traces)	++	
	64-CF	Pyroxenes > Phyllosilicates ≥ Quartz ≫ Hematite (traces) > Magnetite/Maghemite?	+	
	75-CF	Pyroxenes ≫ Quartz ≥ Hematite > Phyllosilicates	+	
	53-CF	Pyroxenes > Quartz > Phyllosilicates > Hematite > Maghemite > Jarosite (traces)	+++	
	52-CF	Pyroxenes > K-Feldspars > Maghemite > Fluorapatite (traces)	++	
	Pre-caldera formations	20-RI	Olivines > Pyroxenes > Phyllosilicates > Quartz > Fluorapatite (traces)	+
		33-AF	Hematite > Pyroxenes ≫ Quartz > Phyllosilicates	+
67-CF		Pyroxenes ≫ Plagioclase > Hematite–Quartz and Phyllosilicates (traces)	+	
11-SF		Pyroxenes > Hematite ≫ Phyllosilicates > Quartz	–	
6-SF		Calcite ≫ Quartz > Fluorapatite > Phyllosilicates ≈ K-Feldspars > Anatase > Pyroxenes ≈ Rutile	–	

predominates. In the yellow topsoil (55-CF Y) quartz and traces of plagioclase were also identified by XRD. In the red topsoil (55-CF R) jarosite was found in addition to hematite and phyllosilicates. This mineralogical composition, particularly the presence of hypogene jarosite is expected due to the most recent volcanic eruption with the occurrence of sulfur-rich fumaroles (Kula and Baldwin, 2011). Jarosite was also detected by XRD in sample 53-CF (volcanic conduit, before 1721).

4.3. Iron speciation

Mössbauer spectra (selected examples in Figs. 3–5) were fitted to sextets and doublets each corresponding to an Fe containing phase or to a set of unresolved contributions from Fe-bearing phases. Furthermore, assuming similar recoil-free fractions at 4 K, the relative area of each doublet or sextet is proportional to the amount of Fe contributing to it.

In all spectra taken at room temperature (Figs. 3–5) doublets with isomer shift $IS \sim 0.35\text{--}0.42$ mm/s and quadrupole splitting $QS \sim 0.56\text{--}0.97$ mm/s are observed (Table 3). They are typical in soil spectra corresponding to Fe^{3+} in silicates, namely phyllosilicates and pyroxenes (McCammon, 1995), and nanoparticle oxides which are superparamagnetic at 295 K (Coe, 1988; Murad, 1998; Vandenberghe et al., 2000). In samples 53-CF (volcanic conduit, before 1721) and 55-CF R (MG crater, 1995) an additional Fe^{3+} doublet with QS (1.14–1.19 mm/s), significantly larger than those of the silicate and nanoparticle Fe^{3+} oxides is observed. This doublet reveals the presence of jarosite (Gracia et al., 1990; Maia et al., 2012; Murad, 1998) in agreement with XRD data. The doublets with the highest $IS = 1.03\text{--}1.14$ mm/s and QS , characteristic of high-spin Fe^{2+} are also found and are attributed to ferrous iron in silicate phases, namely phyllosilicates and pyroxenes (McCammon, 1995). Sextets corresponding to microcrystalline Fe oxides (particles large enough

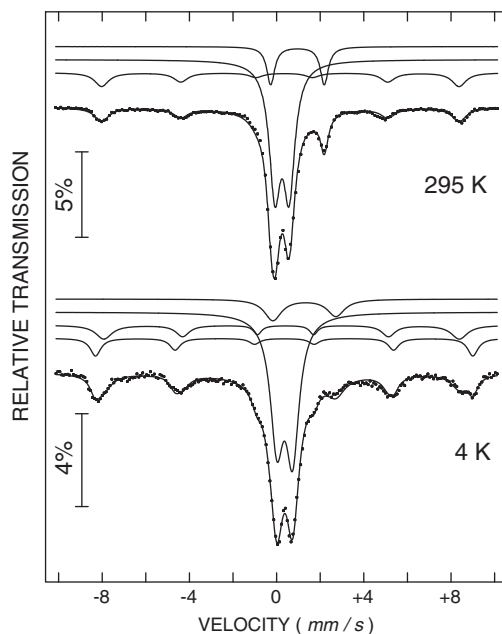


Fig. 3. Mössbauer spectra of 6-SF topsoil (parent rock: carbonatite with ~4 Ma) of Fogo island (Cape Verde), taken at 295 and 4 K.

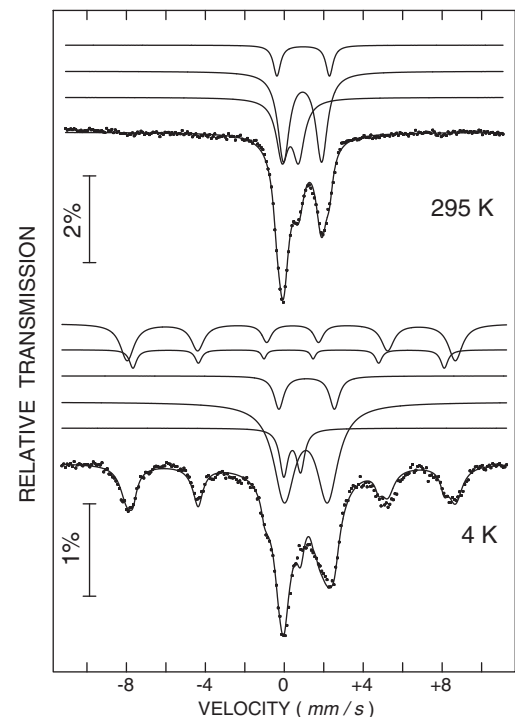


Fig. 4. Mössbauer spectra of 52-CF topsoil (parent rock: pyroclasts before 1721) of Fogo island (Cape Verde), taken at 295 and 4 K.

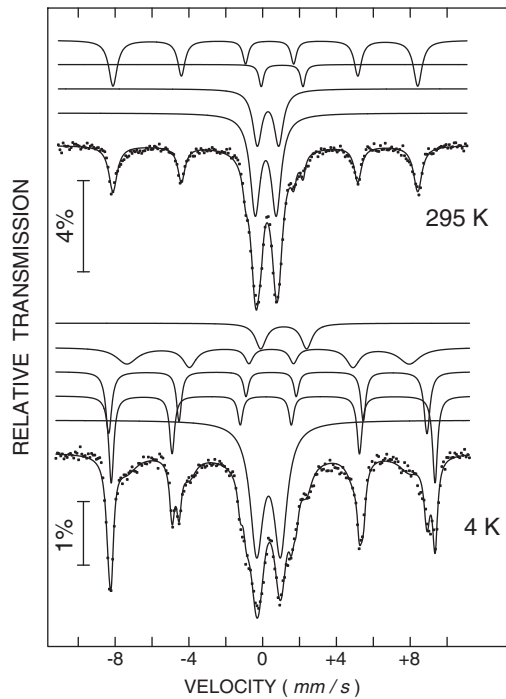


Fig. 5. Mössbauer spectra of 55-CF R topsoil (parent rock: pyroclasts of Mota Gomes crater – 1995 eruption) of Fogo island (Cape Verde), taken at 295 and 4 K.

to give rise to a magnetic hyperfine splitting at 295 K) are also observed. Those with $IS = 0.36\text{--}0.39$ mm/s and quadrupole shift, $\varepsilon \sim -0.20$ mm/s, are typical of hematite. For a few post-caldera topsoils additional sextets with lower IS and $\varepsilon \sim 0$ mm/s which may be due to maghemite are also observed. Three spectra (samples 64-CF, 50-CF and 68-CF, post-caldera 1852–1951) showed a third sextet with $IS = 0.64\text{--}0.66$ mm/s and magnetic hyperfine field $B_{\text{hf}} = 46.1\text{--}47.6$ T, characteristic of $\text{Fe}^{2.5+}$ in magnetite.

In order to estimate the fraction of Fe in oxides, measurements at temperatures as low as 4 K were performed for most samples. Such a low temperature is necessary to ensure that the relaxation of the magnetic moments of all the oxide particles, no matter how small, slows down below the Larmor precession rate of the ^{57}Fe nuclei (3.7×10^7 Hz). In this case the oxide particles are below their blocking temperature and will give rise to a magnetic sextet in the Mössbauer spectra instead of a superparamagnetic doublet, which cannot be resolved from the contribution of paramagnetic Fe^{3+} in silicates. In the 4 K spectra this doublet is still present but with a lower relative area. For each sample the difference in the relative areas of this doublet between 295 and 4 K is, within experimental error, equal to the increase in the relative area of the hematite and/or maghemite sextets. Hematite sextets keep $\varepsilon \sim -0.20$ mm/s showing that this oxide contains impurities and does not undergo the Morin transition keeping the ferrimagnetic state down to 4 K (Vandenberghe et al., 2000). 55-CF R (MG crater, 1995) is the only sample where a well resolved sextet with $\varepsilon \sim 0.4$ mm/s is observed, typical of hematite in the antiferromagnetic state. For some samples hematite sextets have very broad peaks and $\varepsilon \sim 0$ mm/s. These sextets may result from hematite with different crystallinity degrees and impurity contents; some of the particles may have undergone the Morin transition and an average ε is observed. Broad maghemite sextet peaks may also be attributed to different defect or impurity concentrations.

At 4 K jarosite is magnetically ordered. Sextets with IS, B_{hf} and ε (Table 3), typical of jarosite (Bigham and Nordstrom, 2000; Murad, 1998; Vandenberghe et al., 2000) are thus observed in the spectra of 53-CF (volcanic conduit, before 1721) and 55-CF R (MG crater, 1995). The relative areas of these sextets are within experimental error equal to those of the jarosite doublets observed at 295 K.

Sextets with $IS = 0.75\text{--}0.77$ mm/s and $B_{\text{hf}} = 47.6\text{--}49.1$ T, characteristic of $\text{Fe}^{2.5+}$ are also observed in samples 64-CF, 50-CF and 68-CF (post-caldera 1852–1951). These may be explained if magnetite identified in the 295 K spectra of these samples is partially oxidized, which is not surprising, and do not undergo the Verwey transition. In fact according to Bowen et al. (1993) the Verwey transition disappears below 4 K for $\text{Fe}_{3-x}\text{O}_4$ when $x > 0.09$. Doublets with $IS = 1.20\text{--}1.26$ mm/s and with relative areas similar, within experimental error to those estimated for the ferrous Fe doublets at 295 K are also observed. QS of these doublets at 4 K are higher than at 295 K as expected for high-spin Fe^{2+} . The IS of all sextets and doublets increases as the temperature decreases according to the second order Doppler shift.

5. Discussion

5.1. Pre-caldera formations

Mössbauer results show that in topsoils from the pre-caldera formations Fe incorporated in silicates is strongly oxidized and hematite is the only Fe oxide present. Furthermore hematite occurs from poorly to well crystallized, *i.e.* from nano-oxides which only give rise to a sextet in the spectra at 4 K to bulk hematite whose sextet is clearly observed at 295 K (Table 3). The well-crystallized hematite is mainly detected in carbonatite (6-SF) and nephelinite topsoil samples (33-AF and 67-CF). Limburgite and nephelinite topsoils present the highest total Fe contents of all the studied samples (Table 1). They also present the highest degrees of Fe oxidation (Fig. 6) and hematite contents curiously similar to those of the topsoils of the 1995 eruption. The fact that the oldest topsoils are the most oxidized is consistent with their longer exposure to weathering. As already deduced from a study of a paleosol profile developed on volcanic ashes under a semi-arid climate in Fogo island (Marques et al., 2011a,b), oxidation appears to be the major chemical weathering mechanism. The evolution of Fe speciation in the whole sample (<2 mm fraction) through the profile suggests that primary magnetite, when present, is first oxidized to maghemite and finally to hematite. No Fe oxyhydroxides are detected. In a first step Fe^{2+} in the primary silicates is partially oxidized to Fe^{3+} preserving their structure. Eventually, as oxidation proceeds, Fe^{3+} is partly released from the silicate minerals and remobilized as hematite. In this work it is found that the oldest, most weathered, pre-caldera topsoils are also those with the highest total Fe content as expected considering that Fe^{3+} is a conservative element while many others were leached away during the long weathering process (Fig. 6). The Fe content of fresh rock samples from the pre- and post-caldera formations here studied is similar (Marques et al., in preparation) except for the carbonatite where the $\text{Fe}_2\text{O}_3/\text{T}$ is the lowest (app. 1%). The iron enrichment during weathering is thus particularly significant in the topsoil developed on this carbonatite. This topsoil also shows an Fe^{3+} fraction close to 90%, within the highest range of observed values.

5.2. Post-caldera formations

In contrast to the older topsoils where the only Fe oxide detected is micro and nano-crystalline hematite, in several post-caldera topsoils maghemite is observed and in both of the most recent ones, from 1852 and 1951 events, magnetite is also detected. A few topsoils of the pre-historic and historic volcanic conduits (53-CF, 55-CF R) and a pyroclast sample from the 1995 event (55-CF) have jarosite in addition to Fe oxides and Fe containing silicates. Sulfates result largely from the introduction of sulfur-bearing magmatic gases into meteoric water in the upper levels of the volcanoes. In supergene conditions soluble Fe hydroxysulfates, particularly jarosite-group minerals are formed in low-pH surface environments. The presence of jarosite in alkaline topsoils of Fogo island developed on volcanic conduit materials suggests a hypogene origin of this mineral. Hypogene jarosite may be stable at surface environments over decades up to at least a few hundreds of years as in the case of sample 53-CF (volcanic conduit, before 1721). In fact

Table 3

Estimated parameters from the Mössbauer spectra of the topsoil samples from Fogo island (Cape Verde) taken at 295 K and 4 K. IS (mm/s) isomer shift relative to metallic α -Fe at 295 K; QS (mm/s) quadrupole splitting. $\varepsilon = (e^2V_{zz}Q/4) (3\cos^2\theta - 1)$ (mm/s) quadrupole shift estimated for the sextets. B_{hf} (Tesla) magnetic hyperfine field; I relative area. Estimated errors ≤ 0.02 mm/s for IS, QS, ε , <0.2 T for B_{hf} and $<2\%$ for I.

Sample	T	Fe state	IS, mm/s	QS, ε , mm/s	B_{hf} , Tesla	I
6-SF (carbonate)	295 K	Fe ³⁺ silicates/spo	0.37	0.65	–	67%
		Fe ²⁺ silicates	1.08	2.47	–	15%
		Fe ³⁺ α Fe ₂ O ₃	0.36	–0.18	50.8	19%
	4 K	Fe ³⁺ silicates/spo	0.49	0.72	–	59%
		Fe ²⁺ silicates	1.39	2.89	–	12%
		Fe ³⁺ α Fe ₂ O ₃	0.43	–0.18	50.6	16%
		Fe ³⁺ α Fe ₂ O ₃	0.47	–0.01	53.7	13%
67-CF (nephelinite)	295 K	Fe ³⁺ silicates/spo	0.37	0.70	–	69%
		Fe ²⁺ silicates	1.09	2.01	–	10%
		Fe ²⁺ silicates	1.11	2.80	–	7%
	4 K	Fe ³⁺ α Fe ₂ O ₃	0.36	–0.23	50.3	14%
		Fe ³⁺ silicates/spo	0.49	0.90	–	12%
		Fe ²⁺ silicates	1.23	2.80	–	14%
		Fe ³⁺ α Fe ₂ O ₃	0.50	–0.06	44.4	22%
11-SF (nephelinite)	295 K	Fe ³⁺ α Fe ₂ O ₃	0.48	–0.14	49.4	46%
		Fe ³⁺ α Fe ₂ O ₃	0.51	–0.09	53.6	6%
		Fe ³⁺ silicates/spo	0.37	0.71	–	75%
	4 K	Fe ²⁺ silicates	1.07	2.02	–	6%
		Fe ²⁺ silicates	1.10	2.85	–	5%
		Fe ³⁺ Fe ₂ O ₃ relaxation	0.36	–0.07	50.2	8%
		Fe ³⁺ Fe ₂ O ₃ relaxation	0.36	–0.04	44.2	6%
33-AF (nephelinite)	295 K	Fe ³⁺ silicates	0.50	0.74	–	36%
		Fe ²⁺ silicates	1.25	2.75	–	5%
		Fe ²⁺ silicates	1.28	3.13	–	4%
	4 K	Fe ³⁺ α Fe ₂ O ₃	0.47	–0.04	50.4	55%
		Fe ³⁺ silicates/spo	0.37	0.71	–	50%
		Fe ²⁺ silicates	1.14	2.82	–	7%
		Fe ³⁺ α Fe ₂ O ₃	0.38	–0.23	52.0	43%
20-RI (limburgite)	295 K	Fe ³⁺ silicates	0.51	0.70	–	5%
		Fe ²⁺ silicates	1.25	3.04	–	5%
		Fe ³⁺ α Fe ₂ O ₃	0.48	0.02	47.6	60%
	4 K	Fe ³⁺ α Fe ₂ O ₃	0.50	–0.18	53.8	30%
		Fe ³⁺ silicate/spo	0.38	0.71	–	80%
		Fe ²⁺ silicates	1.14	2.91	–	20%
		Fe ³⁺ silicates	0.50	0.74	–	60%
53-CF (pyroclasts volcanic conduit 1721)	295 K	Fe ²⁺ silicates	1.33	3.13	–	16%
		Fe ³⁺ α Fe ₂ O ₃	0.48	–0.15	49.5	24%
		Fe ³⁺ jarosite	0.40	1.19	–	19%
	4 K	Fe ³⁺ silicates/spo	0.41	0.78	–	33%
		Fe ²⁺ silicates	1.06	1.92	–	16%
		Fe ²⁺ silicates	1.05	2.61	–	20%
		Fe ³⁺ γ Fe ₂ O ₃	0.29	–0.07	49.5	5%
52-CF (pyroclasts 1721)	295 K	Fe ³⁺ α Fe ₂ O ₃	0.40	–0.20	51.9	7%
		Fe ³⁺ silicates/spo	0.50	1.07	–	21%
		Fe ²⁺ silicates	1.15	2.03	3.2	18%
	4 K	Fe ²⁺ silicates	1.16	2.80	–	19%
		Fe ³⁺ γ Fe ₂ O ₃	0.41	0.00	48.0	5%
		Fe ³⁺ jarosite	0.49	–0.19	47.4	19%
		Fe ³⁺ α Fe ₂ O ₃	0.50	–0.18	52.9	18%
75-CF (lava 1799)	295 K	Fe ³⁺ silicates/spo	0.42	0.83	–	35%
		Fe ²⁺ silicates	1.04	1.93	–	53%
		Fe ²⁺ silicates	1.07	2.66	–	12%
	4 K	Fe ³⁺ silicates	0.51	0.85	–	9%
		Fe ²⁺ silicates	1.20	2.18	–	50%
		Fe ²⁺ silicates	1.24	2.81	–	10%
		Fe ³⁺ γ Fe ₂ O ₃	0.33	0.00	48.9	6%
72-CF (deposit/lahar post-caldera)	295 K	Fe ³⁺ α Fe ₂ O ₃	0.50	–0.07	51.6	25%
		Fe ³⁺ silicates/spo	0.42	0.80	–	35%
		Fe ²⁺ silicates	1.02	1.96	–	51%
	4 K	Fe ²⁺ silicates	1.07	2.66	–	14%
		Fe ³⁺ silicates/spo	0.41	0.94	–	28%
		Fe ²⁺ silicates	1.14	2.11	–	40%
		Fe ²⁺ silicates	1.14	2.62	–	18%
73-CF (deposit/lahar contemporaneous)	295 K	Fe ³⁺ α Fe ₂ O ₃	0.37	–0.20	44.2	9%
		Fe ³⁺ α Fe ₂ O ₃	0.36	–0.20	50.2	5%
		Fe ³⁺ silicates	0.52	0.78	–	14%
	4 K	Fe ²⁺ silicates	1.24	2.68	–	42%
		Fe ³⁺ α Fe ₂ O ₃	0.48	–0.11	49.6	25%
		Fe ³⁺ α Fe ₂ O ₃	0.49	–0.09	53.1	19%
		Fe ³⁺ silicates/spo	0.41	0.88	–	39%
295 K	Fe ²⁺ silicates	1.07	1.68	–	16%	
	Fe ²⁺ silicates	1.09	2.29	–	28%	

(continued on next page)

Table 3 (continued)

Sample	T	Fe state	IS, mm/s	QS, ϵ , mm/s	B_{hf} , Tesla	I
64-CF (pyroclasts 1852)	4 K	Fe ³⁺ α Fe ₂ O ₃	0.39	-0.22	48.9	9%
		Fe ³⁺ α Fe ₂ O ₃	0.41	0.18	47.1	8%
		Fe ³⁺ silicates	0.52	0.90	-	24%
		Fe ²⁺ silicates	1.25	2.06	-	13%
		Fe ²⁺ silicates	1.25	2.81	-	27%
		Fe ³⁺ α Fe ₂ O ₃	0.47	-0.10	52.5	9%
	295 K	Fe ³⁺ α Fe ₂ O ₃	0.51	-0.12	48.5	27%
		Fe ³⁺ silicates/spo	0.35	0.85	-	59%
		Fe ²⁺ silicates	1.09	2.04	-	16%
		Fe ²⁺ silicates	1.11	2.73	-	5%
		Fe ³⁺ γ Fe ₂ O ₃	0.31	-0.07	49.3	7%
		Fe ^{2.5+} γ Fe ₂ O ₃	0.64	-0.04	46.1	13%
		Fe ³⁺ α Fe ₂ O ₃	0.39	-0.22	51.4	2%
		Fe ³⁺ silicates	0.47	0.96	-	54%
68-CF (lava 1951)	4 K	Fe ²⁺ silicates	1.19	2.22	-	10%
		Fe ²⁺ silicates	1.21	3.04	-	10%
		Fe ³⁺ γ Fe ₂ O ₃	0.41	-0.15	51.1	7%
		Fe ^{2.5+} γ Fe ₂ O ₃	0.75	-0.22	49.0	14%
		Fe ³⁺ α Fe ₂ O ₃	0.49	-0.22	53.6	5%
		Fe ³⁺ silicates/spo	0.41	0.81	-	28%
	295 K	Fe ²⁺ silicates	1.05	1.90	-	21%
		Fe ²⁺ silicates	1.08	2.58	-	13%
		Fe ³⁺ γ Fe ₂ O ₃	0.35	-0.09	47.9	15%
		Fe ^{2.5+} γ Fe ₂ O ₃	0.66	-0.19	43.2	19%
		Fe ³⁺ α Fe ₂ O ₃	0.40	-0.15	50.5	4%
		Fe ³⁺ silicates	0.52	0.95	-	13%
		Fe ²⁺ silicates	1.26	2.00	-	19%
		Fe ²⁺ silicates	1.27	2.97	-	13%
50-CF (lava 1951)	4 K	Fe ³⁺ γ Fe ₂ O ₃	0.39	0.03	50.2	9%
		Fe ^{2.5+} γ Fe ₂ O ₃	0.77	-0.11	47.6	12%
		Fe ³⁺ α Fe ₂ O ₃	0.49	-0.15	53.2	34%
		Fe ³⁺ silicates/spo	0.41	0.79	-	42%
		Fe ²⁺ silicates	1.01	1.93	-	2%
		Fe ²⁺ silicates	1.03	2.48	-	13%
	295 K	Fe ³⁺ γ Fe ₂ O ₃	0.34	-0.12	47.0	24%
		Fe ^{2.5+} γ Fe ₂ O ₃	0.64	0.11	42.7	9%
		Fe ³⁺ α Fe ₂ O ₃	0.39	-0.24	49.6	10%
		Fe ³⁺ silicates	0.51	0.87	-	20%
		Fe ²⁺ silicates	1.23	2.81	-	16%
		Fe ³⁺ γ Fe ₂ O ₃	0.41	-0.06	51.3	24%
		Fe ^{2.5+} γ Fe ₂ O ₃	0.77	-0.13	45.8	10%
		Fe ³⁺ α Fe ₂ O ₃	0.51	-0.20	53.5	30%
54-CF (lava 1995)	295 K	Fe ³⁺ silicates/spo	0.41	0.82	-	34%
		Fe ²⁺ silicates	1.03	2.59	-	13%
		Fe ³⁺ α Fe ₂ O ₃	0.38	-0.21	49.2	53%
	4 K	Fe ³⁺ silicates	0.50	0.92	-	24%
		Fe ²⁺ silicates	1.23	2.76	-	13%
		Fe ³⁺ α Fe ₂ O ₃	0.49	-0.18	53.2	63%
44-SF (lava 1995)	295 K	Fe ³⁺ silicates/spo	0.41	0.79	-	37%
		Fe ²⁺ silicates	1.01	2.54	-	13%
	4 K	Fe ³⁺ α Fe ₂ O ₃	0.37	-0.20	49.0	50%
		Fe ³⁺ silicates	-	-	-	-
55-CF Y (pyroclasts MG crater, 1995)	295 K	Fe ³⁺ α Fe ₂ O ₃	0.37	0.80	-	90%
		Fe ²⁺ silicates	1.02	2.28	-	10%
55-CF R (pyroclasts MG crater, 1995)	295 K	Fe ³⁺ silicates/spo	0.28	1.14	-	41%
		Fe ³⁺ jarosite	0.40	1.16	-	21%
		Fe ²⁺ silicates	1.16	2.26	-	5%
		Fe ³⁺ α Fe ₂ O ₃	0.37	-0.23	51.2	33%
		Fe ³⁺ silicates	0.43	1.29	-	40%
	4 K	Fe ³⁺ jarosite	0.49	-0.17	47.5	18%
		Fe ²⁺ silicates	1.25	2.49	-	6%
		Fe ³⁺ α Fe ₂ O ₃ ferri	0.48	-0.18	53.5	17%
		Fe ³⁺ α Fe ₂ O ₃ af	0.48	0.40	54.4	19%
		Fe ³⁺ silicate/spo	0.36	0.64	-	31%
55-CF (pyroclasts 1995)	295 K	Fe ³⁺ jarosite	0.37	1.18	-	27%
		Fe ²⁺ silicates	1.08	2.06	-	24%
		Fe ³⁺ α Fe ₂ O ₃	0.38	-0.24	50.5	18%
		-	-	-	-	

Spo superparamagnetic Fe oxides.

Fe³⁺ silicates and Fe²⁺ silicates, Fe³⁺ and Fe²⁺, respectively, in the silicates structure.

Fe³⁺ α Fe₂O₃ ferri and Fe³⁺ α Fe₂O₃ af-Fe³⁺ in hematite in the ferrimagnetic and in the antiferromagnetic state, respectively (see text).

Fe³⁺ Fe₂O₃ relaxation-Fe³⁺ in small sized hematite grains, larger than spo already showing broad magnetic peaks at 295 K but not yet large enough to give rise to a well defined sextet with sharp peaks.

Fe³⁺ γ Fe₂O₃, Fe³⁺ jarosite-Fe³⁺ in maghemite and jarosite, respectively.

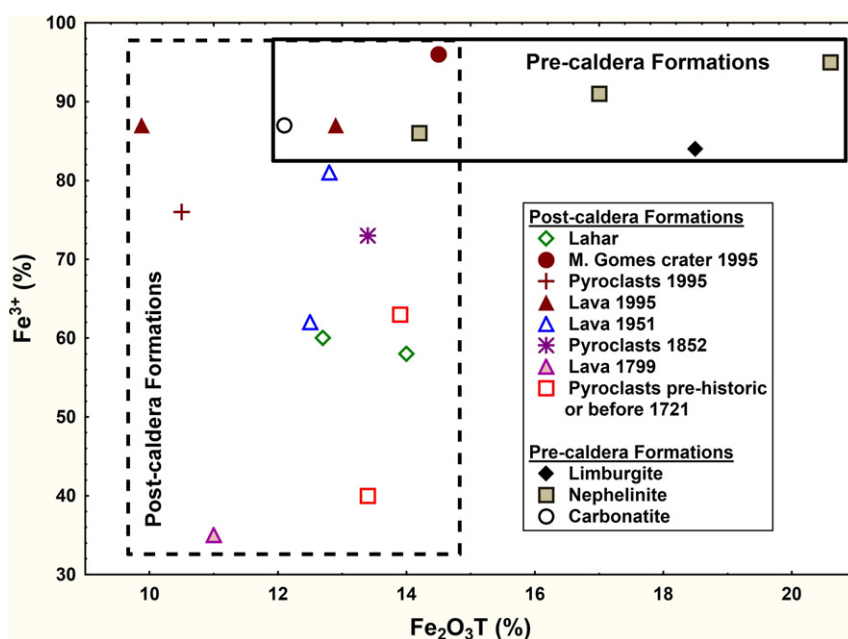


Fig. 6. Total Fe content vs. Fe^{3+} (%) of topsoils of Fogo island (Cape Verde).

jarosite was already found in a Pleistocene aged volcanic ash layer altered under saline-alkaline conditions (lacustrine deposit, Tanzania) far from the accepted stability field for this mineral (McHenry et al., 2012).

It is noteworthy that in general the Fe oxidation degrees of post-caldera formations in topsoils increase from the older to the younger ones (Fig. 6) where they are comparable to those of the pre-caldera formations. Why are the more recent regolith materials the most oxidized surficial samples of the post-caldera formations? Since Mössbauer spectra of the preserved solidified lava samples confirm that the parent rocks have similar oxidation degrees (Waerenborgh et al., in preparation), one possible explanation is the following sequence of events: (i) the outer part of the lavas have a higher glass component which may decompose more rapidly; (ii) Fe is readily oxidized forming small or nanosized particles which may be removed essentially by the wind and other

weathering agents; (iii) after erosion periods of 50–200 years significant amounts of the highly oxidized small particles are removed; and (iv) the inner part of the lava (where Fe is mostly present as Fe^{2+} in silicates such as pyroxenes) is exposed later and more slowly weathered than the former, outer glassy layers. Thus the topsoil of more recent lavas, namely those from 1995, is more oxidized than the topsoils of the exposed inner parts of older historical lavas. Topsoils from pre-caldera formations, although derived from the more weather-resistant inner layers are also strongly weathered since they have been exposed for periods of time several orders of magnitude longer than the post-caldera ones.

Among post-caldera formations differences in total Fe and Fe^{3+} contents due to different exposures to weathering agents are also evidenced (Fig. 6). The significant differences in the two lahar topsoils (72-CF and 73-CF) may also be explained by differences in the material transported downstream during torrential episodes.

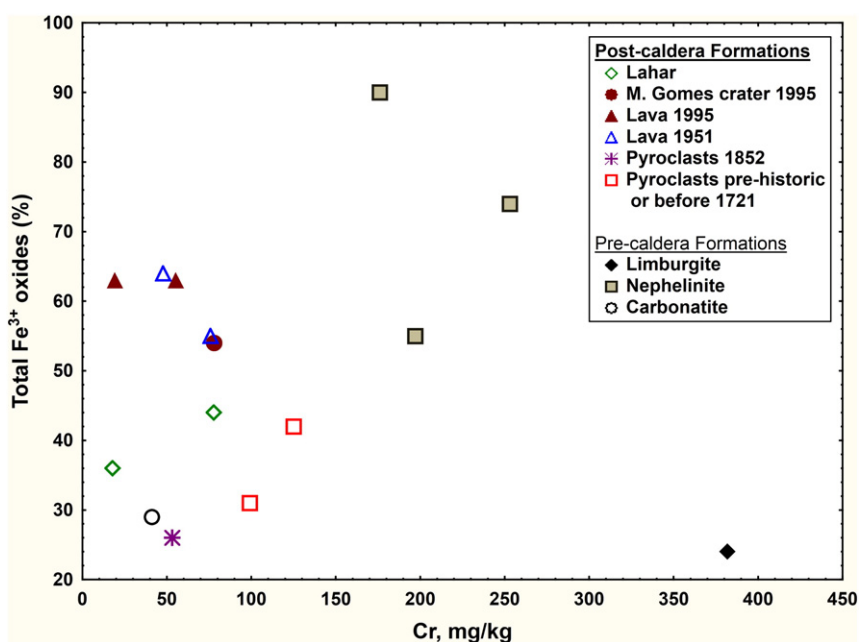


Fig. 7. Chromium content vs. total Fe^{3+} oxides (%) of topsoils of Fogo island (Cape Verde).

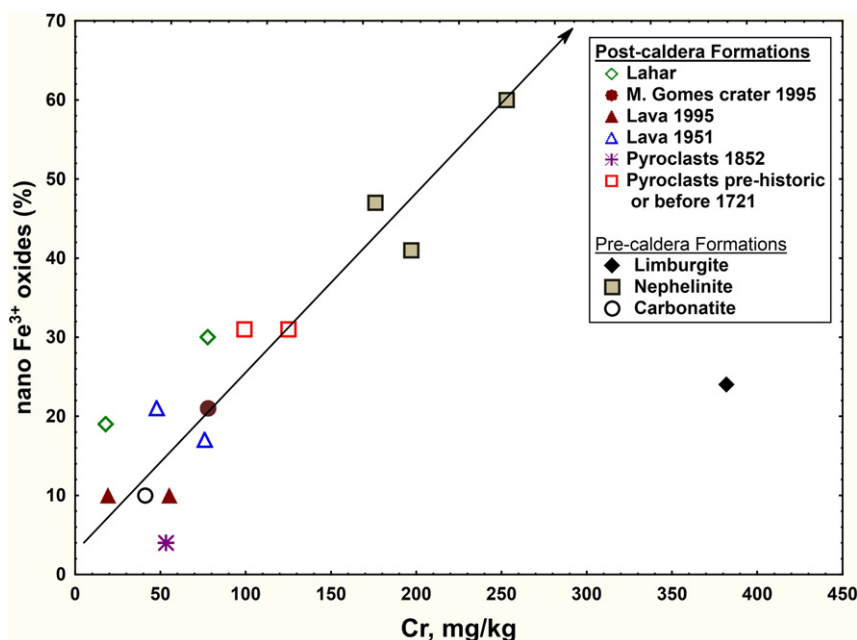


Fig. 8. Chromium content vs. nano Fe³⁺ oxides (%) of topsoils of Fogo island (Cape Verde).

The oxidation degree of the exposed volcanic conduit of Monte Losna where jarosite is found (53-CF, volcanic conduit before 1721) is higher than in the steep slope around the conduit (52-CF, pyroclasts before 1721) where the rain water runs freely instead of accumulating.

In agreement with the higher oxidation degree found for the wetter emplacements of Monte Losna pyroclasts when compared to the drier ones, both 1951 samples show that the emplacement where the annual precipitation is higher (50-CF), iron is more oxidized than in a sample (68-CF) collected in the drier site (Olehowski et al., 2008).

Both topsoil samples (54-CF and 44-SF) of the 1995 lava flow are the most oxidized. The corresponding pyroclastic material on the top of the Mota Gomes crater (sample 55-CF) has a lower degree of oxidation probably due to its higher permeability and therefore shorter time periods where it is in contact with water. Conversely the red pyroclastic material from the inner crater (sample 55-CF R) is the most oxidized material found which may be attributed to its smaller particle size as well as to the hydrothermal activity.

5.3. Cr and As correlation with nanosized Fe oxides

Considering that the total Fe contents of the topsoils do not vary within a large range of values (except for 55-CF Y, the yellow surficial material inside the MG crater), the relative areas of the Fe subspectra corresponding to bulk and nanosized oxides, deduced from the Mössbauer spectra, may be used as a good qualitative estimate of the concentration of these phases. Significant correlations may be found between Cr and As contents and the concentration of Fe oxides (Table 1, Figs. 7 and 8). The highest Cr content is found in limburgite topsoil (20-RI) which is certainly related to the nature of the parent rock namely its high olivine content (De Hoog et al., 2010). Excluding the limburgite topsoil, Cr content increases with the concentration of nano Fe oxides of the samples (Fig. 8). This tendency is already observed, although less clearly, when all iron oxide particle sizes are considered (Fig. 7). Despite the eventual influence of the Cr content of the parent rock, the correlation between Cr content and iron oxides, particularly the nanoparticles, in the studied topsoils of Fogo island is evident. This may be explained by the fact that the adsorption of Cr or even the incorporation of Cr³⁺ substituting for Fe³⁺ in lattice positions should be significantly higher in nanosized than in bulk oxides due to their high specific surface area (Manceau et al., 2000). Therefore the Cr content is much better correlated with the nanosized oxides than with the bulk ones. It should be noted that

nephelinites (11-SF, 33-AF, 67-CF) with the highest Fe fraction in nanosized oxides also have the highest Fe contents. Therefore the increase of the concentration of nanosized oxides relative to the post-caldera samples is actually slightly higher than the Fe fraction in nanosized oxides shown in Fig. 8.

The present results show that Cr content in Fogo island topsoils is not correlated with the grain size. Nevertheless this element is more concentrated in topsoils where iron is more oxidized and remobilized to iron oxides, particularly as nanosized particles of hematite. Marques et al. (2012) found that chromium also occurs in high amounts in topsoils of Santiago (another island of Cape Verde archipelago) independent of the granulometry.

The post-caldera formation topsoil 53-CF (volcanic conduit, before 1721) has a higher Cr concentration than expected considering their nano Fe oxides contents alone. While in the 11-SF (nephelinites, pre-caldera) case referred above this may be associated with a different mineral composition of the parent rock, in the 53-CF case another explanation is necessary. Jarosite is observed in the Mössbauer spectra of sample 53-CF. A large fraction of Fe³⁺ is incorporated in jarosite. If this fraction is added to that in the nano Fe oxides this sample will join the trend observed for the other topsoils. In fact several percent Cr³⁺ substitution for Fe³⁺ in potassium and sodium jarosites may be achieved at temperatures lower than 100 °C (Dutrizac and Chen, 2005). Considering that sample 53-CF has the highest amount of vitreous material, these results suggest that the amorphous phase precipitates rapidly and that partial replacement of Fe³⁺ by Cr³⁺ (in the order of magnitude of mg/kg) may take place in jarosite-group compounds.

Like chromium, arsenic is more concentrated in the pre-caldera topsoils (Table 1). In the post-caldera formations the amount of arsenic is in general nondetectable, except in the volcanic conduits such as in sample 53-CF from Monte Losna and particularly inside the Mota Gomes volcanic crater (55-CF Y, 1995 event) where As concentration reaches 13.5 mg/kg, certainly due to sulfate precipitation following hydrothermal activity (AsO₄³⁻ replacing SO₄²⁻) (Fernández-Martínez et al., 2008; Paktunc and Dutrizac, 2003).

This study has shown that iron phases which may occur in significant amounts in topsoils of Fogo island can play an important role in the retention of other metals. Such a role may also be inferred from the Cr and As behavior observed in topsoils of another island of the Cape Verde archipelago, Santiago island (Marques et al., 2012). The adsorption of a significant fraction of Cr by iron oxides may at least

partially explain the low percentage (~30%) of Cr that was extracted by *aqua regia* from the Santiago island topsoils. Higher arsenic concentrations were found in the finer grain-size fractions of these topsoils. However arsenic was less available in these finer fractions as inferred from *aqua regia* extraction experiments.

6. Conclusion

The detailed Fe speciation performed in topsoils with different granulometry and developed in volcanic materials dated from ~4 Ma to 1995 in the Atlantic Fogo island (Cape Verde archipelago) under semi-arid climate showed the evolution of iron behavior during weathering. Oxidation is a major weathering mechanism. Magnetite is gradually oxidized to hematite. Fe^{2+} in primary pyroxenes and/or olivine is oxidized to Fe^{3+} . When the silicate structure is disrupted Fe^{3+} is remobilized as hematite. No goethite is observed by Mössbauer spectroscopy most probably as a consequence of aridity. The presence of jarosite, the only hydroxide detected in the whole sample of the studied topsoils, may be explained by its hypogene origin and its stability under alkaline surface environments over long periods of time (at least hundreds of years) Nanosized hematite was found to be of great importance in the retention of Cr and As that might be a threat to the environmental health in the volcanic Fogo island.

Acknowledgments

The authors would like to thank the reviewers for comments, suggestions, and corrections that improved the manuscript. Grateful acknowledgements are made to financial support made by the project PEst-C/CTE/UI4035/2011 for the fieldwork, and also to the staff of the Portuguese Research Reactor (RPI) of CTN/IST for their assistance with the neutron irradiations.

References

- Berner, K.B., Berner, R.A., 1996. *Global Environment: Water, Air and Geochemical Cycles*. Prentice Hall, New Jersey, USA.
- Bigham, J.M., Nordstrom, D.K., 2000. Iron and aluminum hydroxysulfate minerals from acid sulfate waters. In: Jambor, J.L., Alpers, C.N., Nordstrom, D.K. (Eds.), *Sulfate Minerals, Crystallography, Geochemistry and Environmental Significance: Mineralogical Society of America. Reviews in Mineralogy and Geochemistry*, 40, pp. 351–403.
- Bowen, H.J.M., 1979. *Environmental Chemistry of the Elements*. Academic Press, London; New York.
- Bowen, L.H., De Grave, E., Vandenberghe, R.E., 1993. Mössbauer effect studies of magnetic soils and sediments. In: Long, G.J., Grandjean, F. (Eds.), *Mössbauer Spectroscopy Applied to Magnetism and Materials Science*, vol.1. Plenum Press, N. York, pp. 115–160.
- Brindley, G.W., Brown, G., 1980. *Crystal Structures of Clay Minerals and their X-ray Identification*. Mineralogical Society, London (495 pp.).
- Brum da Silveira, A., Serralheiro, A., Martins, I., Cruz, J., Madeira, J., Munhá, J., Pena, J., Matias, L., Senos, M.L., 1996. A erupção da Chã das Caldeiras (Ilha do Fogo) de 2 de Abril de 1995. *Orgão do Serviço Nacional de Protecção Civil*. 3–14.
- Brum da Silveira, A., Madeira, J., Munhá, J., Mata, J., Martins, S., Mouro, C., Tassinari, C., 2006. The Summit Depression of Fogo Island (Cape Verde): Caldera and/or Flank Collapse? *International Association of Volcanology and Chemistry of the Earth's Interior (IAVCEI)* 23.
- Cabral Pinto, M.M.S., 2010. *Geochemical Mapping of Santiago Island with a Medium/Low Sampling Density*. (PhD thesis) University of Aveiro, Portugal (410 pp.).
- Carroll, D., 1970. *Rock Weathering*. Plenum Press, New York, USA.
- Chesworth, W., 1992. Weathering systems. In: Martini, I.P., Chesworth, W. (Eds.), *Developments in Earth Surface Processes 2. Weathering, Soils & Paleosols*. Elsevier, pp. 19–38.
- Coey, J.M.D., 1988. Magnetic properties of iron in soil iron oxides and clay minerals. Ch 14 In: Stucky, J.W., Goodman, B.A., Schwertmann, U. (Eds.), *Iron in Soils and Clay Minerals*. Nato ASI Series C, vol.217. D. Reidel Publ. Co., Dordrecht, pp. 397–466.
- Day, S.J., Heleno da Silva, S.I.N., Fonseca, J.F.B.D., 1999. A past giant lateral collapse and present-day flank instability of Fogo, Cape Verde Islands. *J. Volcanol. Geotherm. Res.* 94, 191–218.
- De Hoog, J.C.M., Gall, L., Cornell, D.H., 2010. Trace-element geochemistry of mantle olivine and application to mantle petrogenesis and geothermobarometry. *Chem. Geol.* 270, 196–215.
- Dias, M.I., Prudêncio, M.I., 2007. Neutron activation analysis of archaeological materials: an overview of the ITN NAA laboratory, Portugal. *Archaeometry* 49 (2), 381–391.
- Dung, H.M., Freitas, M.C., Santos, J.P., Marques, J.G., 2010. Re-characterization of irradiation facilities for k_0 -NAA at RPI after conversion to LEU fuel and re-arrangement of core configuration. *Nucl. Inst. Methods Phys. Res. A* 622, 438–442.
- Dutrizac, J.E., Chen, T.T., 2005. Factors affecting the precipitation of chromium(III) in jarosite-type compounds. *Metall. and Materi. Trans. B* 36, 33–42.
- Fernández-Martínez, A., Charlet, L., Cuervo, G.J., Johnson, M.R., Román-Ross, G., Bardelli, F., Turrillas, X., 2008. Arsenate incorporation in gypsum probed by neutron, X-ray scattering and DFT modelling. *J. Phys. Chem. A* 112 (23), 5159–5166.
- Figueiredo, M.O., Silva, L.C., Pereira da Silva, T., Torres, P.C., Mendes, M.H., 1997. *Mineralogia das incrustações resultantes da actividade fumarólica da erupção de 1995 na ilha do Fogo, Cabo Verde. A erupção vulcânica de 1995 na ilha do Fogo, Cabo Verde*. IICST. ISBN: 972-672-863-0, pp. 187–199.
- Figueiredo, M.O., Silva, T.P., Basto, M.J., Ramos, M.T., Chevallier, P., 1999. Indirect monitoring of heavy metals in volcanic gases by synchrotron X-ray microprobe (μ -SRXRF) qualitative analysis of sublimates. *J. Anal. At. Spectrom.* 14 (3), 505–507.
- Formoso, M.L.L., 2006. Some topics on geochemistry of weathering: a review. *An. Acad. Bras. Cienc.* 78 (4).
- Gauthier-Lafaye, F., Taieb, F., Paquet, R., Chahi, H., Prudêncio, M.I., Sequeira Braga, M.A., 1993. Composition isotopique de l'oxygène de palygorsquites associées à des calcrètes: conditions de formation. *Compte Rendue de l'Academie de Sciences de Paris*, t 316, Série II, pp. 1239–1245.
- Gordon, S.J., Dorn, R.I., 2005. Localized weathering: implications for theoretical and applied studies. *Prof. Geogr.* 57 (1), 28–43.
- Gouveia, M.A., Prudêncio, M.I., 2000. New data on sixteen reference materials obtained by INAA. *J. Radioanal. Nucl. Chem.* 245, 105–108.
- Gouveia, M.A., Prudêncio, M.I., Morgado, I., Cabral, J.M.P., 1992. New data on the GSJ reference rocks JB-1a and JG-1a by instrumental neutron activation analysis. *J. Radioanal. Nucl. Chem.* 158, 115–120.
- Govindaraju, K., 1994. Compilation of working values and sample description for 383 geochemical standards. *Geostand. Newslett.* 18, 1–158.
- Gracia, M., Gancedo, J.R., Martínez-Alonso, A., Tascon, J.M.D., 1990. Comparative Mössbauer study of the oxidation of pyrite under different conditions. *Hyperfine Interact.* 58, 2581–2588.
- Heleno da Silva, S.I.N., Day, S.J., Fonseca, J.F.B.D., 1999. Fogo volcano, Cape Verde Islands: seismicity-derived constraints on the mechanism of the 1995 eruption. *J. Volcanol. Geotherm. Res.* 94, 219–231.
- Heleno, S.I.N., Faria, B.V.E., Bandomo, Z., Fonseca, J.F.B.D., 2006. Observations of high-frequency harmonic tremor in Fogo, Cape Verde Islands. *J. Volcanol. Geotherm. Res.* 158, 361–379.
- Holdsen, G.R., Berner, R.A., 1979. Mechanism of feldspar weathering. In: *Experimental studies*. *Geochim. Cosmochim. Acta* 43, 1161–1171.
- Kula, J., Baldwin, S.L., 2011. Jarosite, argon diffusion, and dating aqueous mineralization on Earth and Mars. *Earth Planet. Sci. Lett.* 310, 314–318.
- Le Bas, T.P., Masson, D.G., Holtom, R.T., Grevemeyer, I., 2007. Submarine Mass Movements and Their Consequences. In: Lykousis, V., Sakellariou, D., Locat, J. (Eds.), pp. 337–345.
- Madeira, J., BrumdaSilveira, A., 2005. *Geomorphic and Structural Analysis of the Fogo Island Volcano (Cape Verde)*. Abstract Volume of SAL2005 International Workshop on Ocean Island Volcanism, Sal, Cape Verde.
- Madeira, J., Munhá, J., Tassinari, C.G.C., Mata, J., Brum da Silveira, A., Martins, S., 2005. K/Ar ages of carbonatites from the island of Fogo (Cape Verde). *Actas da XIV Semana da geoquímica e VII Congresso de geoquímica dos países de língua Portuguesa*, pp. 475–478.
- Madeira, J., Brum da Silveira, A., Mata, J., Mourão, C., Martins, S., 2008. The Role of Mass Movements on the Geomorphologic Evolution of Island Volcanoes: Examples from Fogo and Brava in the Cape Verde Archipelago. *Comunicações Geológicas*, 95 93–106.
- Maia, F., Pinto, C., Waerenborgh, J.C., Gonçalves, M.A., Prazeres, C., Carreira, O., Sério, S., 2012. Metal partitioning in sediments and mineralogical controls on the acid mine drainage in Ribeira da Água Forte (Aljustrel, Iberian Pyrite Belt, Southern Portugal). *Appl. Geochem.* 27, 1063–1080.
- Manceau, A., Schlegel, M.L., Musso, M., Sole, V.A., Gauthier, C., Petit, P.E., Trolard, F., 2000. Crystal chemistry of trace elements in natural and synthetic goethite. *Geochim. Cosmochim. Acta* 64, 3643–3661.
- Marques, R., Prudêncio, M.I., Rocha, F., Ferreira da Silva, E., 2010. Geochemistry and mineralogy of volcanic soils from Ocean Fogo island (Cape Verde). 19th World Congress of Soil Science, Soil Solutions for a Changing World, Brisbane, Australia, pp. 102–105.
- Marques, R., Prudêncio, M.I., Waerenborgh, J.C., Rocha, F., Dias, M.I., Ferreira da Silva, E., 2011a. Geochemistry and mineralogy of volcanic ash red paleosol from Fogo island (Cape Verde). *Mineral. Mag.* 75 (3), 1408.
- Marques, R., Prudêncio, M.I., Waerenborgh, J.C., Rocha, F., Dias, M.I., Ferreira da Silva, E., 2011b. Iron and other chemical elements in a paleosol developed on volcanic ash in Fogo Island (Cape Verde). *Proceedings of the VIII Cong. Ibérico de Geoquímica (Castelo Branco, Portugal)*, 1, pp. 411–416.
- Marques, R., Prudêncio, M.I., Rocha, F., Cabral Pinto, M.S., Silva, M.M.V.G., Ferreira da Silva, E., 2012. REE and other trace and major elements in the topsoil layer of Santiago island, Cape Verde. *J. Afr. Earth Sci.* 64, 20–33.
- McCammion, C.A., 1995. Mössbauer spectroscopy of minerals. In: Ahrens, T.J. (Ed.), *Mineral Physics and Crystallography: a Handbook of Physical Constants*. Amer. Geophys. Union, Washington, D.C., pp. 332–347.
- McHenry, L.J., Chevrièr, V.F., Schröder, C., 2012. Spatial vs. temporal distribution of K-jarosite in a saline-alkaline paleolake deposit: implications for the distribution and longevity of jarosite on Mars. 43rd Lunar and Planetary Science Conference, The Woodlands, Texas (LPI Contribution No. 1659, id.2010. <http://www.lpi.usra.edu/meetings/lpsc2012/pdf/2010.pdf>).
- Meunier, A., 2003. *Argiles*. Contemporary Publishing International – GB Science Publisher, Paris.
- Mota Gomes, A., 2006. A problemática da Geologia e dos Recursos Hídricos na Ilha do Fogo. Relatório inédito, Praia, Cabo Verde.

- Munsell, 1998. Soil Color Charts. Revised washable edition. (New Windsor, NY).
- Murad, E., 1998. Clays and clay minerals: what can Mössbauer spectroscopy do to help understand them? *Hyperfine Interact.* 117, 39–70.
- O'Day, P.A., 2006. Chemistry and mineralogy of arsenic. *Elements* 2, 77–83.
- Olehowski, C., Naumann, S., Fischer, D., Siegmund, A., 2008. Geo-ecological spatial pattern analysis of the island of Fogo (Cape Verde). *Glob. Planet. Chang.* 64, 188–197.
- Paktunc, D., Dutrizac, J.E., 2003. Characterization of arsenate-for-sulfate substitution in synthetic jarosite using X-ray diffraction and X-ray absorption spectroscopy. *Can. Mineral.* 41, 905–919.
- Prudêncio, M.I., 2009. Ceramic in ancient societies: a role for nuclear methods of analysis. In: Koskinen, Axel N. (Ed.), *Nuclear Chemistry: New Research*. Nova Science Publishers, Inc., New York, pp. 51–81.
- Prudêncio, M.I., Sequeira Braga, M.A., Paquet, H., Waerenborgh, J.C., Pereira, L.C.J., Gouveia, M.A., 2002. Clay minerals assemblages in weathering basalt profiles from central Portugal: climatic significance. *Catena* 49 (1–2), 77–89.
- Prudêncio, M.I., Gonzales, M.I., Dias, M.I., Galán, E., Ruiz, F., 2007. Geochemistry of sediments from El Melah lagoon (NE Tunisia): a contribution for the evaluation of anthropogenic inputs. *J. Arid Environ.* 69, 285–298.
- Prudêncio, M.I., Dias, M.I., Ruiz, F., Waerenborgh, J.C., Duplay, J., Marques, R., Franco, D., Ben Ahmed, R., Gouveia, M.A., Abad, M., 2010. Soils in the semi-arid area of the El Melah Lagoon (NE Tunisia) — variability associated with a closing evolution. *Catena* 80, 9–22.
- Prudêncio, M.I., Dias, M.I., Waerenborgh, J.C., Ruiz, F., Trindade, M.J., Abad, M., Marques, R., Gouveia, M.A., 2011. Rare earth and other trace and major elemental distribution in a pedogenic calcrete profile (Slimene, NE Tunisia). *Catena* 87, 147–156.
- Summons, R.E., 1993. Biogeochemical cycles: a review of fundamental aspects of organic matter formation, preservation, and composition. In: Engel, M.H., Macko, S.A. (Eds.), *Organic Geochemistry — Principles and Applications*. Plenum Press, New York, pp. 3–18.
- Torres, P.C., Madeira, J., Silva, L.C., Brum da Silveira, A., Serralheiro, A., Mota Gomes, A., 1998. Carta geológica da ilha do Fogo (República de Cabo Verde). Erupções históricas e formações enquadantes. LATEX, Departamento de Geologia da Fac. de Ciências da Univ. de Lisboa. Escala 1–25000.
- Vandenbergh, R.E., Barrero, C.A., da Costa, G.M., Van San, E., De Grave, E., 2000. Mössbauer characterization of iron oxides and (oxy)hydroxides: the present state of the art. *Hyperfine Interact.* 126, 247–259.
- Vaughan, D.J. (Ed.), 2006. *Sulfide Mineralogy and Geochemistry. Reviews in Mineralogy and Geochemistry*. Mineralogy Society of America (714 pp.).
- Waerenborgh, J.C., Rojas, D.P., Vyshatko, N.P., Shaula, A.L., Kharton, V.V., Marozau, I.P., Naumovich, E.N., 2003. Fe^{4+} formation in brownmillerite $\text{CaAl}_0.5\text{Fe}_{0.5}\text{O}_{2.5} + \delta$. *Mater. Lett.* 57, 4388–4393.